Proceedings of the ASME 28th International Conference on Ocean, Offshore and Arctic Engineering
OMAE2009
May 31 - June 5, 2009, Honolulu, Hawaii, USA

OMAE2009-79052

CFD SIMULATION OF WAVE RUN-UP ON A SEMI-SUBMERSIBLE AND COMPARISON WITH EXPERIMENT

Bogdan Iwanowski*
FORCE Technology Norway AS
Claude Monets alle 5
1338 Sandvika
Norway
Email: boi@force.no

Marc Lefranc
FORCE Technology Norway AS
Email: mrl@force.no

Rik Wemmenhove
FORCE Technology Norway AS
Email: riw@force.no

ABSTRACT

Use of CFD tools for industrial offshore applications is a common practice nowadays. So is the need for validation of such tools against experimental results. This paper presents one of the CFD tools, ComFLOW, which solves Navier-Stokes equations and employs an improved Volume of Fluid (iVOF) method to find temporary location of fluid's free surface.

The code is used to simulate flow around a semi-submersible offshore platform due to an incoming regular wave. In particular, wave run-up on the semi's columns and under-deck fluid impact phenomena are investigated on high-accuracy computational grids with number of cells being in range of 10 millions.

Results of numerical simulations are compared with experimental data and focus is on local fluid flow details in immediate vicinity of the platform. Wave run-up on the platform's columns and fluid pressures at various locations, including under-deck impact, are reported and verified against the experiment for a range of incoming wave heights.

INTRODUCTION

Design of an offshore structure requires accurate estimation of an extreme wave elevation in order to fulfill requirements of the positive air gap below the platform deck. For structures that have columns of a large size, such as semi-submersibles or gravity based platforms, it is also necessary to take into account local amplifications of the wave elevation along the platform's columns, a non-linear phenomenon known as run-up. A proper estimation of the wave run-up must go beyond the linear wave diffraction theory.

The problem has been addressed in the offshore-related bibliography, [1–4]. The proposed methods include higher-order potential solutions, particle image velocimetry (PIV) experiments and fully non-linear CFD calculations with either Level-Set (LS), Volume of Fluid (VOF) or Smooth Particle Hydrodynamics (SPH) approaches used to track movement of the fluid's free surface. An interesting discussion can be found in [4], where the CFD method discussed here, the ComFLOW code, has been compared with the 2^{nd} order diffraction theory application, the widely known WAMIT program.

Main topic of this paper is presentation of ComFLOW numerical simulations' results of the wave run-up along legs of a semi-submersible platform. The CFD results are confronted with data obtained from model experiments of the platform, for regular incoming waves.

THE COMFLOW PROGRAM

The 3D CFD solver ComFLOW has been developed by University of Groningen, The Netherlands. It introduces a local height function as an improvement over the original VOF algorithm [5]. The code has been continuously and actively developed within Joint Industry Projects SAFE-FLOW (2001-2004) and ComFLOW-2 (2005-2008).

*Address all correspondence to this author.

MATHEMATICAL MODEL

The single-phase version of the ComFLOW program is used in this paper, and it is understood that the considered fluid is incompressible and viscous (put it simply, the sea water), while void fills remaining space of the computational domain.

The fluid flow can be found by solving continuity equation, Eqn. (1), together with Navier-Stokes equations describing conservation of momentum, Eqn. (2):

$$\nabla \cdot \mathbf{u} \;=\; 0 \tag{1}$$

where $\mathbf{u} \;=\; (u,v,w)$ is fluid's velocity vector.

$$\frac{\partial \mathbf{u}}{\partial t} \;+\; \mathbf{u} \cdot \nabla \mathbf{u} \;=\; -\frac{1}{\rho} \nabla p \;+\; \frac{\mu}{\rho} \nabla \cdot \nabla \mathbf{u} \;+\; \mathbf{G} \tag{2}$$

with p being fluid's pressure, ρ its constant density and μ its constant dynamic viscosity coefficient. Further, t is time and $\mathbf{G} \;=\; (G_x, G_y, G_z)$ is an external body force, for example gravity.

In VOF-like methods a function $F(x,y,z,t)$ is introduced, with values between zero and one, to indicate fractional volume of a computational cell which is occupied by fluid. Evolution of the VOF function is given by Eqn. (3):

$$\frac{\partial F}{\partial t} \;+\; (\mathbf{u} \cdot \nabla)\, F \;=\; 0 \tag{3}$$

These are the most basic set of partial differential equations solved numerically by ComFLOW.

Boundary conditions imposed on surface of a body are of the no-slip kind ($\mathbf{u} = 0$). More detailed description of free-surface boundary conditions, discretization of the equations and time integration scheme used in ComFLOW can be found in [6, 7], where the local height function concept is also discussed.

THE SEMI-SUBMERSIBLE MODEL EXPERIMENTS

The semi-submersible model experiments were performed by MARIN of The Netherlands at their basin in Wageningen. Main objective of these experiments was to provide a validation material for the ComFLOW code and the experiments themselves were part of the ComFLOW-2 JIP.

A photograph of the semi-submersible model is shown in Fig. (1). The model scale was rather typical, 1:50. Main dimensions of the semi-submersible platform (full scale) are displayed in Fig. (2).

The experimental program conducted by MARIN was quite extensive, and a complete description can be found in [8]. Three regular incoming waves (hereafter nick-named as Short, Medium, Long, with respective periods of 9.0, 11.0 and 13.0 seconds) have been chosen for numerical analysis with ComFLOW and these results will be presented in this paper.

Figure 1. Experimental model, semi-submersible

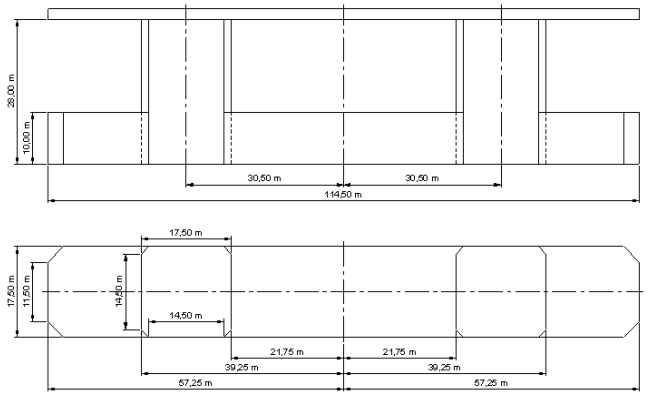

Figure 2. Main dimensions of the test semi-submersible, full scale

REPRESENTATIVE INCOMING WAVE

The experimental basin at MARIN has dimensions of $200 \times 4 \times 3.6$ [m] (length×breadth×water depth) and the semi-submersible platform model was built to the scale of 1:50. It follows that the full scale CFD computational domain would have to be $10000 \times 200 \times 180$ [m].

Currently it is not feasible to computationally reproduce the entire model basin (and perhaps there is a little sense to do that). Therefore, the experimental wave elevation time signal which describes the incoming waves (the signal taken from preliminary wave calibration tests) has been analyzed in order to establish a *representative* incoming wave parameters. It has been decided that the *representative* incoming wave should be of Stokes 5^{th} order type, since steepness of the experimental incoming waves was rather high (0.0573, 0.0739 and 0.0729 for the Short, Medium and Long waves, respectively). Procedure of establishing the *representative* incoming wave is illustrated in graphs, Figs. (3-8) for the Long wave case (T=13.0 [sec]).

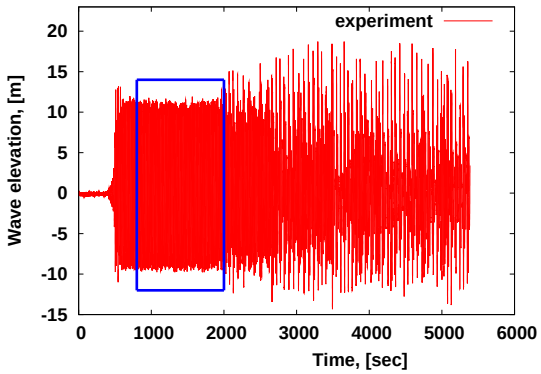

Figure 3. Complete experimental time trace

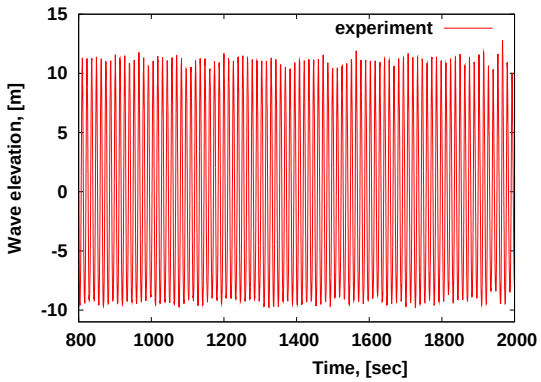

Figure 4. Experimental time trace within a selected time window

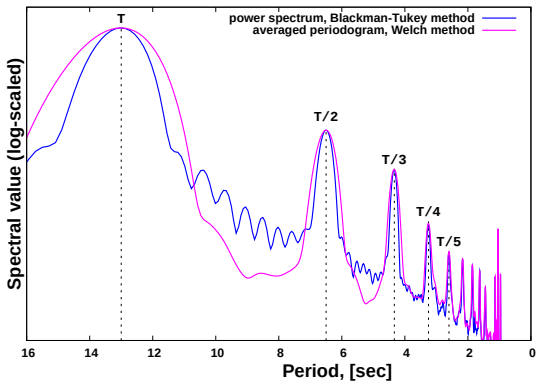

Figure 5. Spectral properties of the wave elevation signal

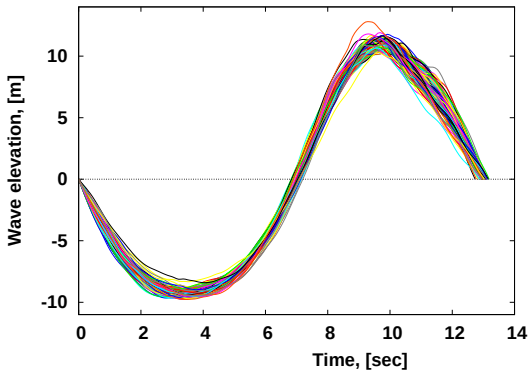

Figure 6. Wave profiles mapped to a common start

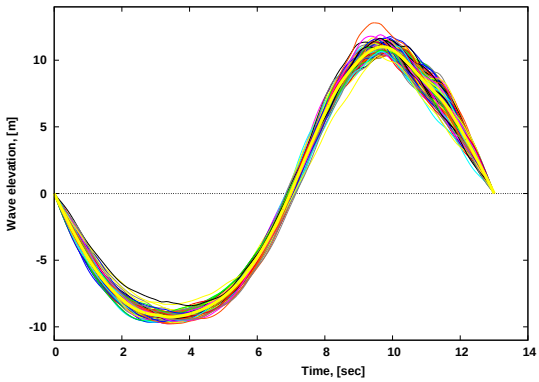

Figure 7. Common-start wave profiles scaled to an average period

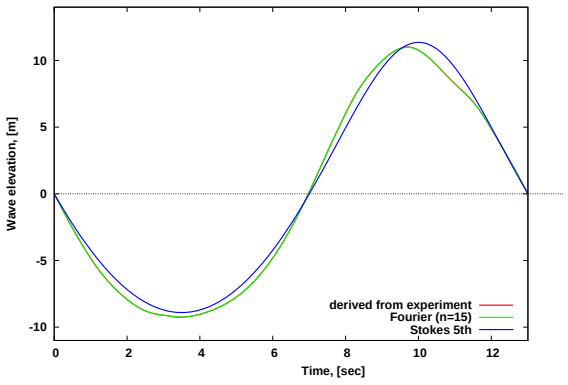

Figure 8. Final incoming wave profile (see also text)

The procedure is described as follows.

1. The entire incoming wave elevation signal is shown in Fig. (3). It can be seen that the wave elevation is stable only until reflections from the far side of the basin start to contaminate the signal. An appropriate time window from the wave elevation signal have been chosen, which includes the stable part only (blue rectangle in Fig. (3).
2. The wave elevation signal within the (stable) window is displayed in Fig. (4).
3. A spectral analysis has been performed on the wave elevation signal within the stable time window (to make the algorithm's description complete: for the spectral analysis' purposes, the original signal has been sub-windowed with the Blackman window). It was hoped to establish numbers and relative significance of dominant peaks in the wave elevation signal spectrum. A simple regular wave model, such as Airy, Stokes 2^{nd}, 3^{rd} or 5^{th} order could then be discovered and implemented in a straightforward manner. But it can be seen in Fig. (5) that the wave elevation spectrum contains much more than five peaks (here, please note that this graph employs a logarithmic scale in order to reveal as many spectral features as possible). The first five harmonics of the fundamental wave period are clearly marked. Displayed graphs are Blackman-Tukey power spectrum and Welch averaged periodogram (these methods use data averaging and are arguably the most convenient for analysis, [9]). No additional data smoothing was applied to obtain the graphs.
4. As described above, it was not possible to (easily) model the incoming waves based on the spectral analysis of the wave elevation signal. The next trial was to collect all waves from the selected time window and map them to a common start. This is shown in Fig. (6). Some scatter of the experimentally recorded wave periods can be observed.
5. The common-start wave profiles have been further scaled to an average wave period. The mapped and scaled profiles and the resulting averaged wave (shown in a yellow colour) can be seen in Fig. (7).
6. The averaged wave profile (the thick yellow-colour curve in Fig. (7) was then subjected to a harmonic analysis in order to get Fourier components of the derived shape. The final Stokes 5^{th} order wave was obtained with a least squares fit to the multi-component Fourier profile. The final Stokes 5^{th} order wave is presented in Fig. (8) as the blue curve (the red and green curves do overlap in this graph).

The above procedure is more exhaustively described and illustrated in [10], for the two other waves which are discussed in this paper (Short, Medium).

Parameters of the *representative* incoming waves derived from the experimental signals are listed in Tab. (1).

Table 1. *Representative* incoming waves, analysis results

Wave	wave parameters (assigned)		wave parameters (from analysis)	
	H	T	H	T
Short	8.0	9.0	7.608	9.006
Medium	15.0	11.0	15.007	11.010
Long	20.0	13.0	20.459	13.005

COMFLOW COMPUTATIONAL SETUP

The presented simulation results have been obtained for ComFLOW computational models having the following features:

(a) fluid flow domain included only the platform's neighbourhood of a reasonable size. The platform model was placed at origin of the coordinate system. The computational domain length was defined as $x = -aL, \ldots, aL$, where L is the *representative* incoming wave length. The a parameter has been set to $a = 1.5$, 1.2, 1.0 for the Short, Medium, Long waves, respectively. Such domain is symmetrical in the longitudinal direction, with the same amount of space upstream and downstream of the platform.
(b) computational domain width was set to 166.67 m (that is, 2/3 of the experimental basin width), and was symmetrical with respect to the platform's symmetry plane. This has been done in order to decrease number of necessary computational cells.
(c) computational domain depth was set to 60 m (that is, 1/3 of the experimental basin depth). Again, the reason was to limit number of the computational cells. There was also an excess of computational cells above the free surface.
(d) the computational grid has been non-uniform away from the body and stretched towards the semi-submersible. The immediate platform's neighbourhood has been covered by a uniform grid. Grid spacing in the uniform grid zone was the same in all three spatial directions and has been set to $\Delta = 0.5$ [m]. Such grid is of high accuracy, in particular with respect to main dimensions of the platform itself, Fig. (2).
(e) the initial fluid configuration (initial condition for the ComFLOW simulation) was that of a fully developed wave field. The *representative* waves were modelled as Stokes 5^{th} order waves, with the "sign correction" implemented [11, 12].
(f) at inlet, $x = -aL$, wave inflow boundary conditions were imposed. The downstream boundary conditions at outflow, $x = aL$, were of Sommerfeldt type.
(g) the fluid flow was simulated for 3-4 wave periods.

Table 2. Description of ComFLOW computational grids

Wave	*representative* wave parameters			ComFLOW grid and total number of cells
	H	T	L	
Short	7.61	9.01	130.75	474×146×121 $\Longrightarrow$ 8 373 684
Medium	15.01	11.01	199.57	548×146×121 $\Longrightarrow$ 9 680 968
Long	20.46	13.00	277.91	612×146×121 $\Longrightarrow$ 10 811 592

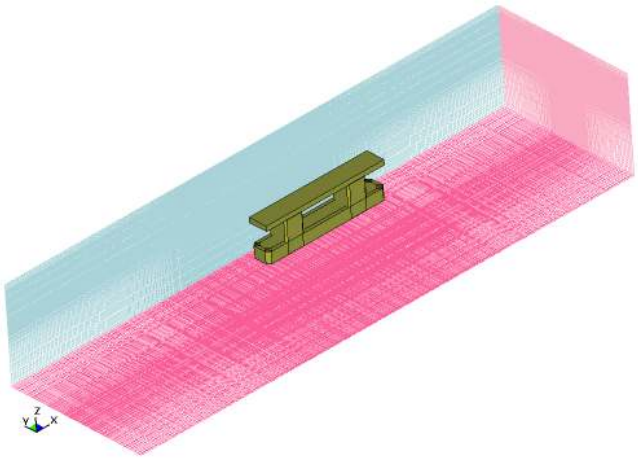

Figure 9. ComFLOW computational domain and grid, Medium wave

Particulars of the used ComFLOW computational grids are listed in Tab. (2), where lengths of the *representative* incoming waves were found from the Stokes 5^{th} order wave theory.

An example of the ComFLOW computational domain is displayed in Fig. (9), for the Medium wave.

It can be seen in Tab. (2) that numbers of the used computational cells were quite substantial (8-11 million cells). The computer CPU times necessary to complete the calculations were substantial as well (115h, 195h and 296h of calculations for the considered wave cases, respectively). The quoted CPU times are for a machine equipped with an AMD Opteron 2218, 2.6 GHz processor.

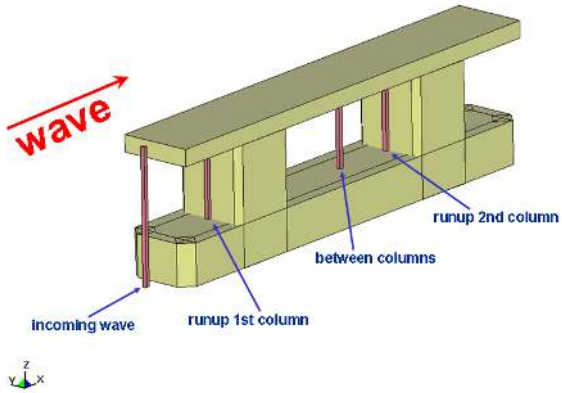

Figure 10. Locations of wave elevation probes

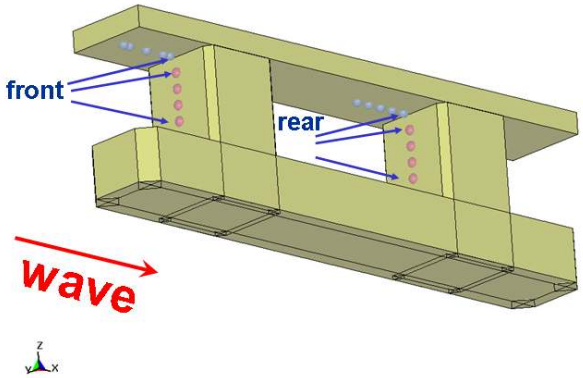

Figure 11. Locations of fluid pressure sensors

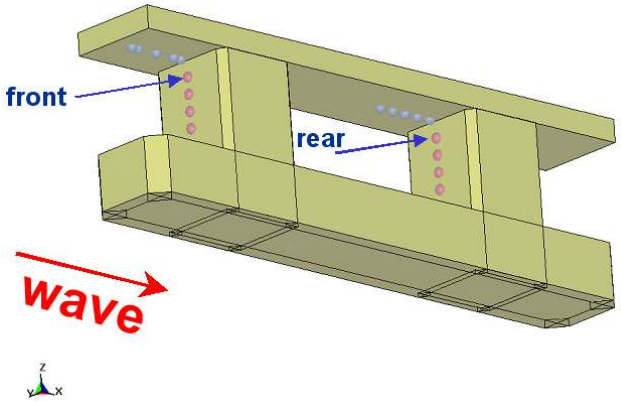

Figure 12. Locations of fluid run-up velocity control points

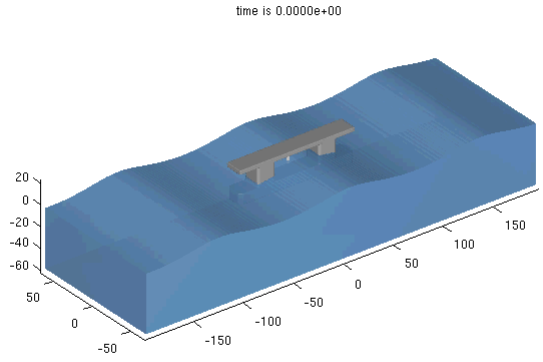

Figure 13. Start of simulation, Short wave

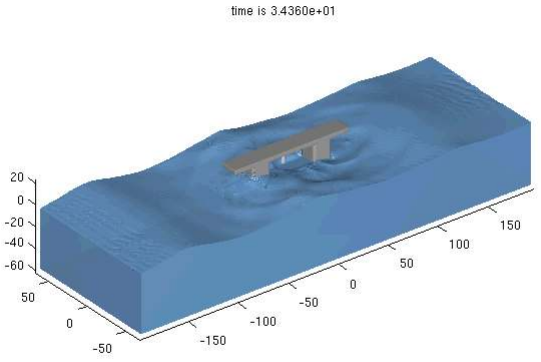

Figure 14. Diffraction pattern, Short wave, entire domain

Monitoring of the ComFLOW Simulation Results

The computed fluid flow parameters were monitored at the same locations where the experimental sensors were placed. The following data will be reported in more detail:

1. fluid height (wave elevation) at 4 locations, Fig. (10).
   (a) incoming wave location (probe ahead of the platform),
   (b) run-up on the 1^{st} column,
   (c) between the columns,
   (d) run-up on the 2^{nd} column.
2. fluid pressure at 6 locations, Fig. (11):
   (a) bottom of the columns (front and rear),
   (b) top of the columns (front and rear),
   (c) under-deck near-column corner (front and rear).
3. fluid run-up velocity (z-component), at 2 locations, top of the columns (front and rear), Fig. (12).

RESULTS

Presentation of the ComFLOW simulation results starts with fluid flow imagery. A simulation starts with the initial fluid configuration of a fully developed wave field, Fig. (13), the example shows the Short wave case. The following image displays the same computational case at end of the simulation, Fig. (14). The wave diffraction patterns due to the platform's presence are clearly visible. Similar diffraction patterns are present for the Medium and Long waves.

Wave run-up along the platform's front column is visualised in four spectacular Figs. (15-18), where results for the Long wave are displayed.

Results, Wave Elevation

Numerical results of the fluid height (wave elevation) are presented for the Medium wave. It can be seen in Fig. (19) that the experimental signal and the ComFLOW result agree quite well at the incoming wave fluid height probe location. ComFLOW reproduces the incoming wave crest height very satisfactorily, but there are differences for the wave troughs. Fluid heights (measured and computed) for both columns and for the probe located between the columns show very good agreement indeed, Figs. (20-22). The fluid height curves contain flat parts (upper extrema) which indicate that the fluid has made contact with the platform's under-deck surface.

Results, Fluid Pressures

The fluid pressure results are given for the Long wave case. The time-pressure graphs are presented for all six pressure sensor locations displayed in Fig. (11).

The experimental and computational results agree very well at bottom points of the semi-submersible columns, Figs. (23-26). But these spots are considered as relatively "easy", since the fluid flow dynamics is not at its extreme there, and a hydrostatic part of the fluid pressure exists.

The two pairs of graphs showing pressures at top locations of the semi's columns, Figs. (24-27), and at the column-underdeck corners, Figs. (25-28), deserve more detailed comments. The respective curves are similar, since locations of the respective pressure sensors are pretty close; Fig. (11) can be consulted again.

It should be emphasized that the first pressure peak in these graphs is not a perfectly reliable result (although the experiment vs. computation agreement is quite good). The fluid flow simulation starts from a fully developed wave field, Fig. (13),

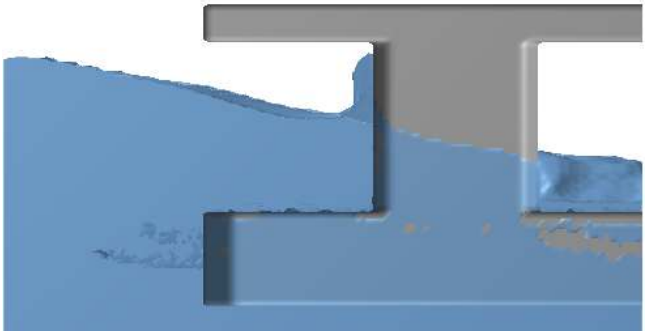

Figure 15. Long wave, the 1^{st} column run-up, stage (a)

Figure 16. Long wave, the 1^{st} column run-up, stage (b)

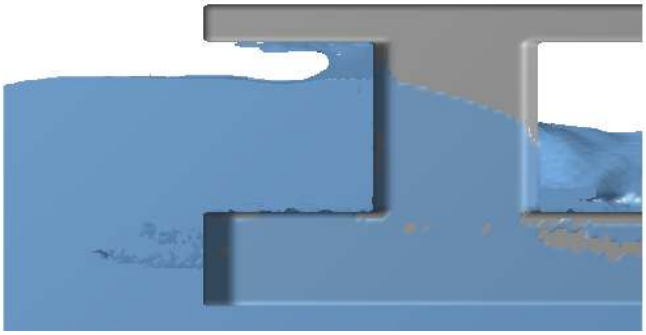

Figure 17. Long wave, the 1^{st} column run-up, stage (c)

Figure 18. Long wave, the 1^{st} column run-up, stage (d)

and there are no diffracted waves around the semi-submersible platform present (yet). The wave diffraction patterns do appear (and presumably are correctly developed), only when the second (then third, fourth, etc.) wave passes the platform's location. Therefore, the wave-body interaction during the first ComFLOW-simulated wave period should be taken with a dose of criticism.

The measured and computed pressure values, displayed in Figs. (24-28), show a pretty reasonable agreement with the experiment (even if the first pressure peak is dismissed from the analysis, see the arguments above).

Results, Upward Run-up Fluid Velocities

No experimental data is available for comparison with the fluid run-up velocities (the velocities were not measured during the experiments). Nevertheless, the computed run-up velocities (vertical components) along the semi-submersible platform's columns are shown for all waves discussed in the paper. Values obtained at the selected control points, see Fig. (12), are displayed. The computed run-up fluid velocities are in a range of 10-20 [m/sec] and can be used to estimate loads on smaller structural elements which are not included into overall model of the semi-submersible platform.

CONCLUSIONS

1. The ComFLOW program can be applied for numerical simulation of wave run-up on a marine structure. An accurate computational grid is necessary to carry out a successful simulation. Unfortunately this leads to substantial computational times.
2. The simulation results compare fairly well with the experiments.
3. All reasonably similar problems (with a similar geometry of the object and with incoming waves having comparable parameters) can also be successfully simulated. The necessary grid accuracy can be found by relating its size to a characteristic dimension of the currently analyzed structure.
4. The computationally demanding CFD simulations seem to be necessary in order to capture the highly non-linear flow features of the wave run-up.

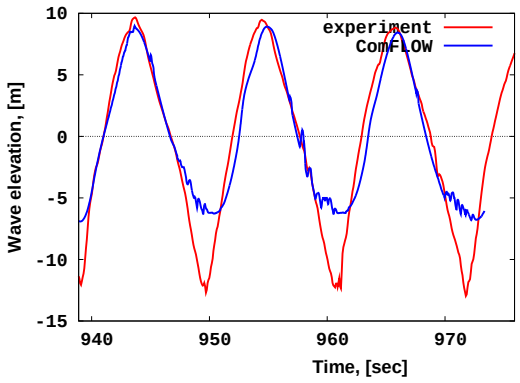

Figure 19. Wave elevation, incoming, Medium wave

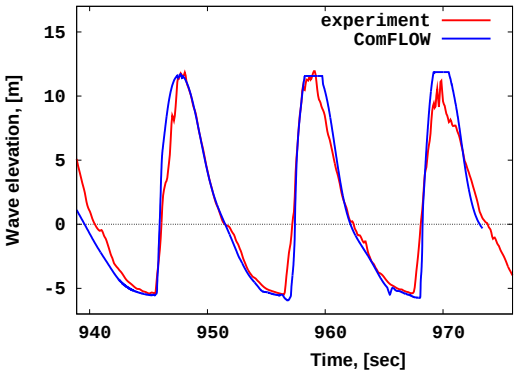

Figure 21. Wave elevation, between the columns, Medium wave

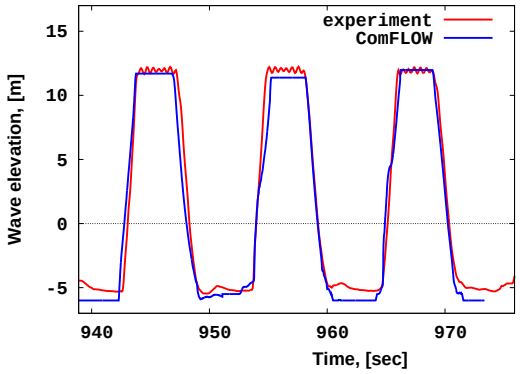

Figure 20. Wave elevation, run-up on the 1^{st} column, Medium wave

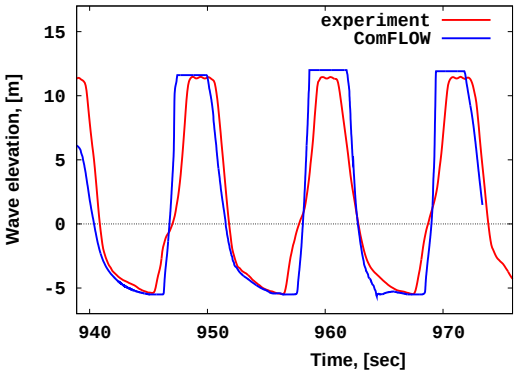

Figure 22. Wave elevation, run-up on the 2^{nd} column, Medium wave

5. The reported CFD simulations took many days to complete. Parallelization of the ComFLOW code is currently under way and should alleviate the problem.

ACKNOWLEDGMENT

Authors would like to thank participants of the ComFLOW-2 Joint Industry Project for financial support and permission to publish the results.

Appendix A: Synchronised Video Frames, Experiment and Calculations

The discussed semi-submersible experiments have been filmed with an analog (rather old-style) camera. A video animation from each of ComFLOW simulations presented in the paper was produced as well. The Appendix shows three time-synchronised video frames composed from the experiment and the calculation, one frame for each of the discussed Short, Medium, Long waves.

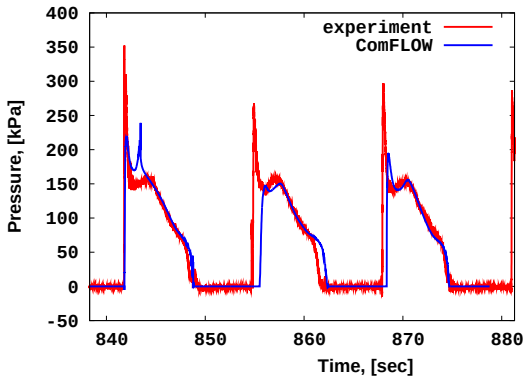

Figure 23. Long wave pressures, the 1^{st} column, bottom

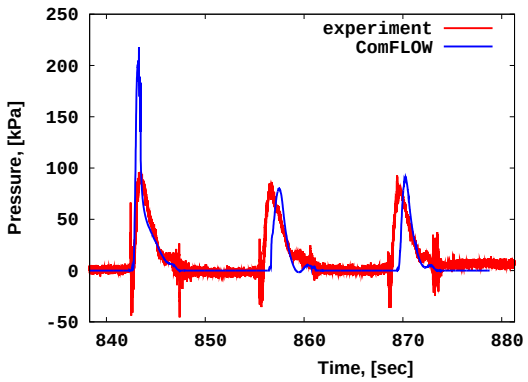

Figure 24. Long wave pressures, the 1^{st} column, top

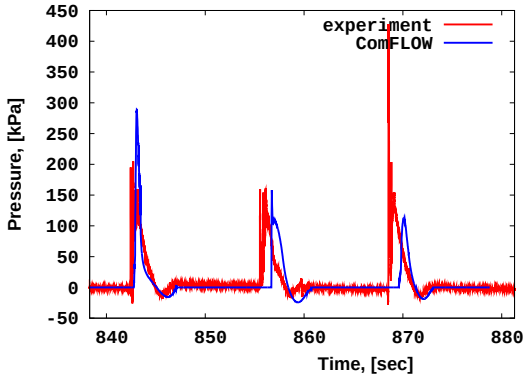

Figure 25. Long wave pressures, the 1^{st} column, under-deck point

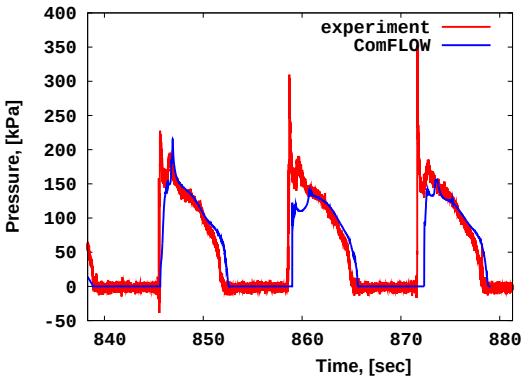

Figure 26. Long wave pressures, the 2^{nd} column, bottom

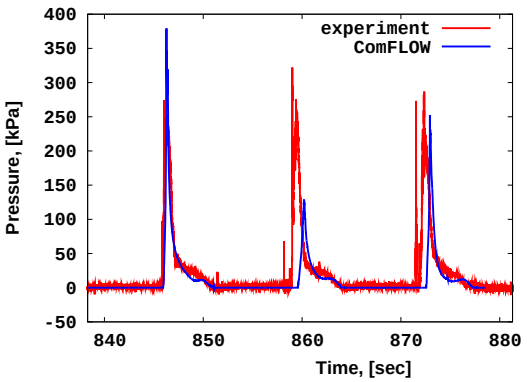

Figure 27. Long wave pressures, the 2^{nd} column, top

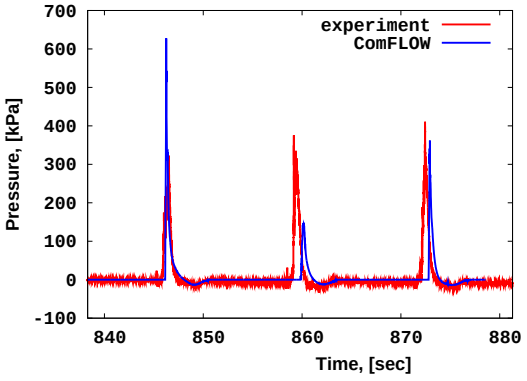

Figure 28. Long wave pressures, the 2^{nd} column, under-deck point

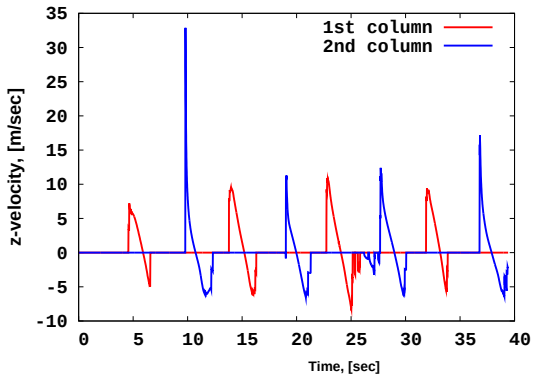

Figure 29. Run-up velocity at top of columns, Short wave

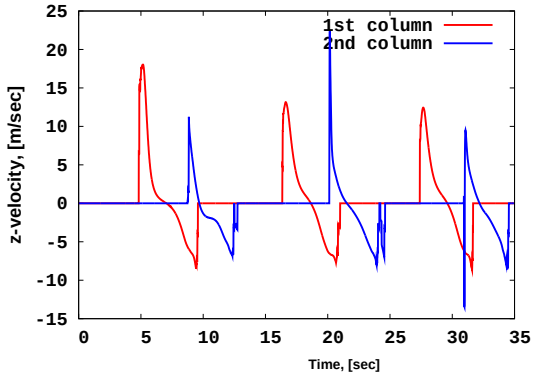

Figure 30. Run-up velocity at top of columns, Medium wave

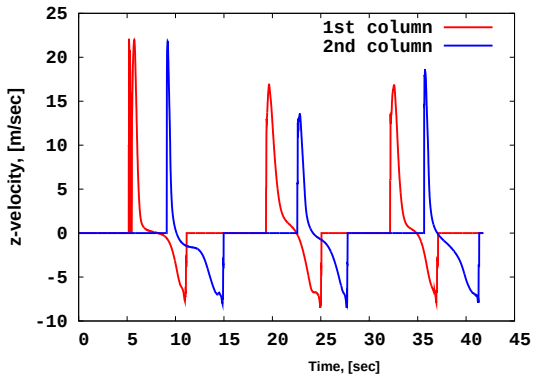

Figure 31. Run-up velocity at top of columns, Long wave

REFERENCES

[1] Buchman, B., Ferrant, P., and Skourup, J., 2000. "Run-up on a Body in Waves and Current. Fully Nonlinear and Finite-order Solutions". *Applied Ocean Research,* **22**, pp. 349–360.

[2] Loots, E., and Buchner, B., 2004. "Wave Run Up As Important Hydrodynamic Issue For Gravity Based Structures". In Proceedings, 23-rd International OMAE Conference, Vancouver, Canada. Paper OMAE2004-51084.

[3] Kristiansen, T., Baarholm, R., Rørtveit, G.J., Hansen, E.W., and Stansberg, C.T., 2005. "Kinematics in a Diffracted Wave Field: Particle Image Velocimetry (PIV) and Numerical Models". In Proceedings, 24-th International OMAE Conference, Halkidiki, Greece. Paper OMAE2005-67176.

[4] Danmeier, D.G., Seah, R.K.M., Finnigan, T., Abault, A., Vache, M., and Imamura, J.T., 2008. "Validation of Wave Run-up Calculation Methods for a Gravity Based Structure". In Proceedings, 27-th International OMAE Conference, Estoril, Portugal. Paper OMAE2008-57625.

[5] Hirt, C.W., and Nichols, B.D., 1981. "Volume Of Fluid (VOF) Method for the Dynamics of Free Boundaries". *Journal of Computational Physics,* **39**, pp. 201–225.

[6] Kleefsman, K.M.T., 2005. "Water Impact Loading on Offshore Structures - A Numerical Study". PhD Thesis, University of Groningen, The Netherlands, November.

[7] Kleefsman, K.M.T., Fekken, G., Veldman, A.E.P., Buchner, B., and Iwanowski, B., 2005. "A Volume-Of-Fluid Based Simulation Method for Wave Impact Problems". *Journal of Computational Physics,* **206**, pp. 363–393.

[8] Bunnik, T.H.J., 2007. Wave Runup Tests on a Semi Submersible. Technical Report 18378-2-HT, Maritime Research Institute Netherlands (MARIN), Wageningen, The Netherlands, September.

[9] Lim, J.S., and Oppenheim, A.V. (Eds)., 1988. *Advanced Topics in Signal Processing*. Prentice-Hall, Englewood Cliffs, NJ.

[10] Iwanowski, B., 2008. ComFLOW-2 JIP: Benchmarks of the ComFLOW Program. Technical Report TR-2008-0049, FORCE Technology Norway AS, Sandvika, Norway, October.

[11] Skjelbreia, L., and Hendrickson, J.A., 1960. "Fifth Order Gravity Wave Theory". In Proceedings, 7-th Coastal Engineering Conference, The Hague, pp. 184–196.

[12] Fenton, J.D., 1985. "A Fifth-Order Stokes Theory for Steady Waves". *Journal of Waterway, Port, Coastal and Ocean Engineering,* **111**(2), pp. 216–234.

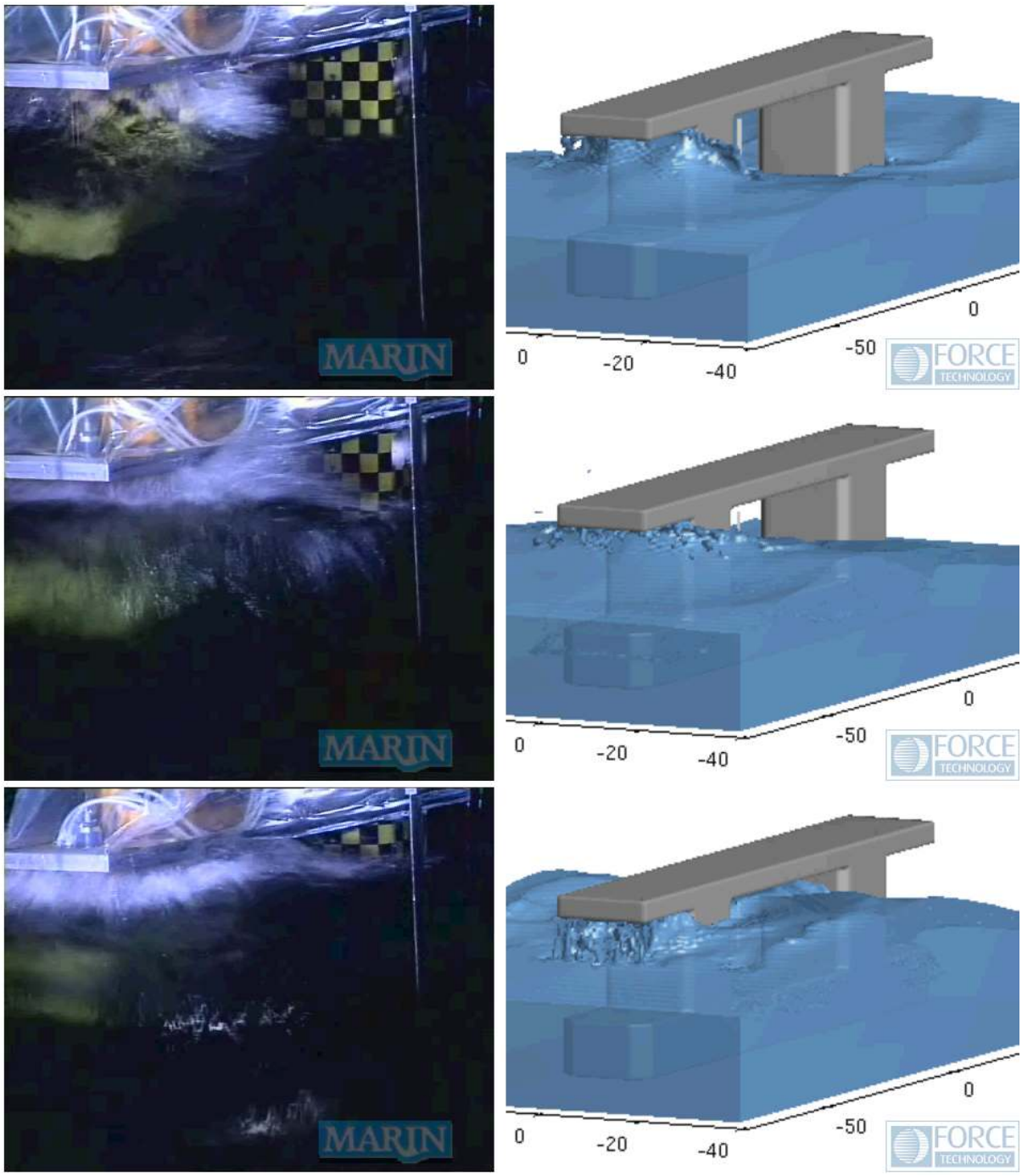

Figure 32. Synchronised video frames, from top: Short, Medium, Long wave